8

In Situ Probing of Oxygen-containing Groups on Acid-treated Carbon Nanofibers using Aromatic Molecules

Hiromasa Nishikiori, Satoshi Kubota, Nobuaki Tanaka,
Morinobu Endo, and Tsuneo Fujii
Shinshu University
Japan

1. Introduction

Development of chemical nanotechnology to control the structure of materials on a nanosize scale is necessary in order to obtain certain physical and chemical properties of the nanomaterials. Carbon nanofibers (CNFs) (Oberlin et al., 1976; Endo, 1988; Endo et al., 2001) are very large multi-walled carbon nanotubes and are technologically easier and economically more favorable to produce than individual single- or double-walled carbon nanotubes (Iijima, 1991; Iijima & Ichihashi, 1993). The CNFs are valuable materials for electronic, mechanical, and optical devices because of their unique structural and quantum characteristics that are similar to small-sized carbon nanotubes (Oberlin et al., 1976; Endo, 1988; Endo et al., 2001; Endo et al., 2002; Yang et al., 2003; Wang et al., 2005; Tan et al., 2006). For practical use, such carbon nanomaterials need to be well dispersed throughout other raw materials. An example of this is the incorporation of carbon nanomaterials into plastics or ceramics, which provide practical materials with well-defined shape and increased strength. Composites of matrices with dispersed carbon nanotubes have been prepared by the polymerization of a polyimide under sonification (Park et al., 2002) and by the sol−gel reaction of a system containing a relatively large amount of N,N′-dimethylformamide as the starting material (Hongbinget al., 2004). However, carbon nanomaterials have a high specific surface area and easily aggregate. Surface functionalization of the carbon nanomaterials is an effective method to disperse them throughout various media for producing new functional materials, which utilize their unique characteristics (Zhu et al., 2003; Gao et al., 2005; Singh et al., 2005). In order to functionalize these carbon nanomaterials one must treat their surface with acids or other chemicals. Treatment of the carbon nanomaterials with nitric acid and sulfuric acid leads to the oxidation of their surface that forms oxidized groups such as −COOH and −C=O within the graphene sheet (Liu et al., 1998; Hamon et al., 2001; Hamon et al., 2002). Generally, the surface functional groups of the modified CNFs are characterized by IR or Raman spectroscopy. It is, however, difficult to obtain quantitative information of the chemical species existing in a monolayer or only a few layers of the oxidized surface of the CNFs using these analyses.

We have previously shown that observing the fluorescence spectra of 1-naphthol (1-NP) is a useful probe on a molecular level for studying the physicochemical properties of the

Source: Nanofibers, Book edited by: Ashok Kumar,
ISBN 978-953-7619-86-2, pp. 438, February 2010, INTECH, Croatia, downloaded from SCIYO.COM

surrounding environment around the 1-NP (Suzuki et al., 1977; Fujii et al., 1995). Based on these investigations, significant physicochemical information of the CNF surface was obtained by in situ spectrometry using 1-NP as a fluorescent probe (Nishikiori et al., 2004; Kubota et al., 2005a; Kubota et al., 2005b). Our unique procedure to create a highly disperse system of CNFs throughout solvents allowed these observations even though the fluorescence of aromatic molecules adsorbed on carbon materials has scarcely been observed due to strong quenching. In this procedure, 1-NP was adsorbed on the untreated CNFs and acid-treated CNFs and they were then dispersed in solvents (Nishikiori et al., 2004; Kubota et al., 2005a). Two types of 1-NP fluorescence, the ^1L_b fluorescence (Suzuki et al., 1977; Fujii et al., 1992) and the ion-pair fluorescence (Mishra et al., 1991; Fujii et al., 1992), were observed from the following two adsorbed forms. These are generated by the π−π interaction between 1-NP and the graphene sheet (Chen et al., 2001b; Long & Yang, 2001) and the hydrogen-bonding interaction between 1-NP and proton-accepting groups the oxidized groups, such as –COOH (–COO-) and –C=O (Nishikiori et al., 2004; Kubota et al., 2005a; Kubota et al., 2005b), generated at the acid-treated CNF surface (Hammon et al., 2002; Lakshminarayanan et al., 2004).

1-Aminopyrene (1-AP) is a Brönsted base and is expected to interact with acidic groups on a solid surface (Hite et al., 1986; Miller et al., 2005). Therefore, oxygen-containing functional groups produced on the surface of the acid-treated CNFs, especially acidic groups such as –COOH (Chen et al., 2001a; Kahn et al., 2002), are characterized by the fluorescence measurements using 1-AP as a molecular probe (Nishikiori et al., 2008). 1-AP is suitable as a fluorescence probe since its spectrum drastically changes with the acid-base equilibrium compared with those of aminonaphthalene or aminoanthracene.

However, unlike the 1-NP species, the low-polar species fluorescence is not observed from the 1-AP species on the graphene sheet of the CNFs. This is because the polar amino group prevents the π−π interaction between the pyrene ring and graphene sheet (Nishikiori et al., 2008) even though pyrene derivatives without amino group are adsorbed onto the CNTs by this interaction (Chen et al., 2001; Tomonari et al., 2006). Therefore, the fluorescence observation of the pyrene adsorbed on the surface of CNFs presents the information of the π−π interaction between the pyrene ring and graphene sheet (Tanigaki et al., 2007).

In this chapter, we will report that in situ fluorescence measurements using aromatic probe molecules are useful for studying the physicochemical properties on the CNF surface. The relationship between the CNF dispersion throughout the solution of the probe molecules and their adsorption onto the CNFs will be discussed by analyzing the UV-visible absorption and fluorescence spectra of the suspension containing the probe molecules and the untreated or acid-treated CNFs.

2. Acid treatment of carbon nanofibers

The CNFs (VGCF, vapor grown carbon fiber) having a diameter ca. 200 nm, a length of ca. 10−20 μm and a surface area of ca. 15 m^2g^{-1}, were provided by Showa Denko Co, Ltd. (Endo et al., 2001). Functionalization of the CNF surfaces was carried out in two ways with liquid acid, as reported in the literature (Liu et al., 1998; Hamon et al., 2001; Hamon et al., 2002, Nishikiori et al., 2004; Kubota et al., 2005b). The first was by refluxing the CNFs in concentrated nitric acid at 393 K for 1 or 24 h followed by rinsing them with copious amounts of water and allowing them to dry at room temperature under vacuum. For a stronger treatment procedure, the CNFs were sonicated in a concentrated H_2SO_4/HNO_3

mixture (3/1 in volume) at 313 K for 24 h. They were then refluxed in a mixture of concentrated sulfuric acid and 30% aqueous hydrogen peroxide (4/1 in volume) at 343 K for 24 h and were refluxed in concentrated nitric acid at 393 K for 24 h. They were then rinsed with copious amounts of water until the washings were confirmed neutral using a pH test paper and allowed to dry at room temperature under vacuum. Designation is held throughout this chapter as the following: Untreated CNFs (N-CNF); CNFs treated solely with nitric acid for 1 and 24 h (A1-CNF and A24-CNF, respectively); CNFs treated with both sulfuric and nitric acids (AA-CNF).
The SEM images and IR spectra of these samples have been described elsewhere (Kubota et al., 2005b). The surface structures of the three CNF samples were hardly distinguished even by their TEM images as previously reported (Toebes et al., 2004; Lakshminarayanan et al., 2004).

3. Quantitative characterization of surface adsorption sites of carbon nanofibers by in-situ fluorescence measurement using 1-naphthol

3.1 Adsorption characteristics of 1-NP on N-CNF

The N-CNF (1.0 mg) was dispersed in aqueous solutions of 1-NP (10 cm^3) by ultrasonic irradiation for 120 h. The 1-NP concentrations ranged from 5×10^{-5} to 5×10^{-4} mol dm^{-3}. The resulting suspensions were centrifuged to remove any precipitates. The absorption and fluorescence spectra of the resulting transparent suspensions were measured.
Figure 1 shows the fluorescence spectra of 1-NP observed in aqueous suspensions including the N-CNF prepared at different initial concentrations of 1-NP, and the resulting Langmuir isotherm for the adsorption of 1-NP on the N-CNF. The fluorescence originating from the ^1L_b state and anion of 1-NP were observed at around 330−350 and 460 nm, respectively (Fujii et al., 1992; Nishikiori et al., 2004). The ^1L_b fluorescence indicates that 1-NP exists in a nonpolar environment as a result of the π−π interaction with the CNF surface (Chen et al., 2001a; Long & Yang, 2001; Nishikiori et al., 2004). Almost all the 1-NP molecules in water exist as neutral species in the ground and the anion species in the excited states because the values of pK_a are 9.2 and 0.4 in their states, respectively (Fujii et al., 1992; Nishikiori et al., 2004). The intensity of the ^1L_b fluorescence relative to that of the anion fluorescence decreases with an increase in the 1-NP concentration, i.e., the ratio of 1-NP in the liquid phase becomes higher, indicating that the adsorption approaches saturation. The total concentration of 1-NP, C, is written as

$$C = [N] + [NF], \tag{1}$$

where N and NF are 1-NP existing in the liquid phase and on the CNF surface by a π−π interaction, respectively. The ratio of the fluorescence intensity of N, I_N, to that of NF, I_{NF}, is defined as R_1. The desorption in the excited states can be ignored because the diffusion rate of molecules is much lower than the fluorescence life time.

$$R_1 = I_N/I_{NF} = A\,[N]/[NF], \tag{2}$$

where A indicates the ratio of the spectroscopic constant of N to that of NF defined by the molar extinction coefficient, ε, and fluorescence quantum yield, Φ.

$$A = \varepsilon_N\Phi_N/\varepsilon_{NF}\Phi_{NF}\ . \tag{3}$$

These equations can be applied to the Langmuir isotherm as follows:

$$\theta = [NF]/[F_1] = K_1[N]/(1+ K_1[N]), \quad (4)$$

where θ is the fractional surface coverage and F_1 is the adsorption site due to the π−π interaction on the N-CNF surface, and K_1 is the adsorption equilibrium constant on the F_1 site. The value $[F_1]$ is the molar amount of the F_1 sites existing on the CNFs dispersed in 1 dm^3 of water. The weight of the dispersed CNFs is about 100 times lower than the initial sampling weight, 1.0 mg, in 10 cm^3 of water.

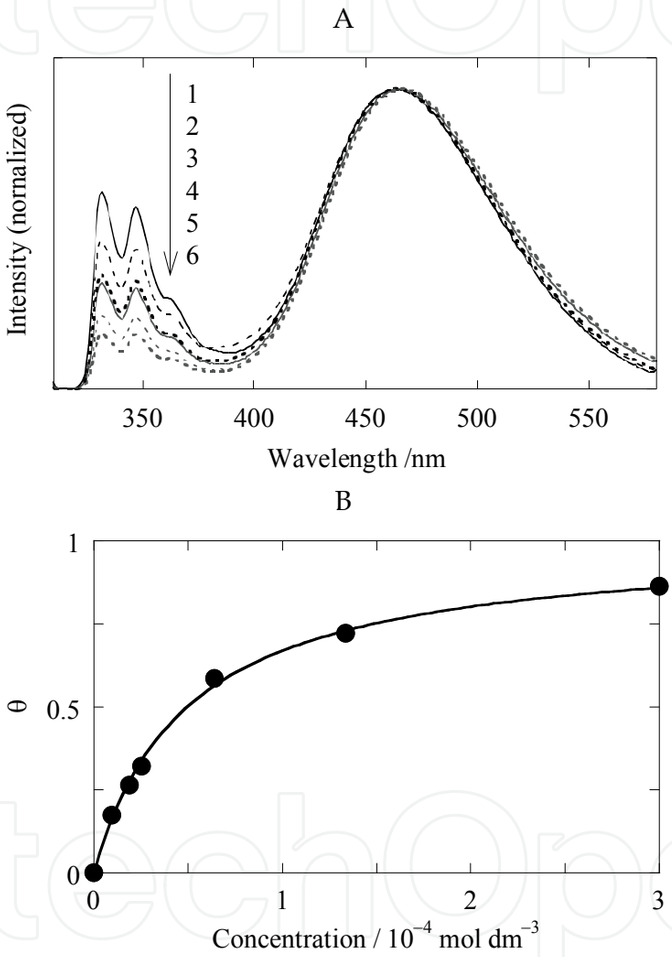

Fig. 1. (A) fluorescence spectra of 1-NP observed in aqueous suspension including N-CNF and (B) resulting Langmuir isotherm for F_1 site. The initial concentrations of 1-NP in water are (1) 5.0×10^{-5}, (2) 8.0×10^{-5}, (3) 1.0×10^{-4}, (4) 2.0×10^{-4}, (5) 3.0×10^{-4}, and (6) 5.0×10^{-4} mol dm^{-3}. The excitation wavelength is 297 nm.

The Langmuir isotherm of 1-NP on the surface of N-CNF was obtained by the curve fitting calculation using the known variables, C and R_1, and the parameters, A, K_1, and $[F_1]$. The experimental and simulated relationships between θ and [N] are plotted in Figure 1B. The experimental values are well-fitted to the Langmuir isotherm. The resulting constants of A, K_1, and $[F_1]$ are summarized in Table 1.

	Spectroscopic constant	Adsorption equilibrium constant / mol^{-1} dm^3
Characters of adsorption sites		
F_1 site	6.5 (*A*)	2.0×10^4
F_2 site (A1-CNF)	1.0 (*B*)	1.7×10^5
F_2 site (A24-CNF)	1.1 (*B*)	2.2×10^5

	F_1 site / mol dm^{-3}	F_2 site / mol dm^{-3}	Total / mol dm^{-3}
Concentration of adsorption sites			
N-CNF	2.3×10^{-4}	0	2.3×10^{-4}
A1-CNF	1.7×10^{-4}	7.4×10^{-5}	2.4×10^{-4}
A24-CNF	1.4×10^{-4}	1.9×10^{-4}	3.3×10^{-4}

Table 1. Constants for CNFs estimated by fluorescence measurements using 1-NP

3.2 Adsorption characteristics of 1-NP on A-CNF

The HNO_3-treated samples, A1-CNF and A24-CNF (1.0 mg) were individually dispersed in aqueous solutions of 1-NP (10 cm^3) by ultrasonic irradiation for 120 h. The 1-NP concentrations ranged from 5×10^{-5} to 5×10^{-4} mol dm^{-3}. The absorption and fluorescence spectra of the resulting transparent supernatants were measured after centrifugation of the suspensions.

Figure 2 shows the fluorescence spectra of 1-NP observed in the A24-CNF suspensions, and resulting Langmuir isotherm for the adsorption of 1-NP on the A24-CNF. The fluorescence band at around 380−450 nm was observed as well as the ^1L_b band. This new band is assigned to the ion pair fluorescence of 1-NP located at the shoulder of the anion band (Mishra et al., 1991; Fujii et al., 1992; Nishikiori et al., 2004). The ion-pair fluorescence indicates that a chemical modification occurred on the CNF surface by the HNO_3 treatment. The ion pair of 1-NP was produced by the hydrogen-bonding interaction between the neutral 1-NP and the oxidized surface of the CNFs (Hamon et al., 2002). The spectral shift in the band from 400 to 440 nm can be observed with an increase in the initial concentration of 1-NP, caused by a decrease in the relative intensity of the ion-pair band and increase in that of the anion band. This phenomenon results from the fact that the adsorption is approaching saturation. On the other hand, the relative intensity of the ^1L_b band increases with an increase in the initial concentration of 1-NP. This result is somewhat strange considering the adsorption equilibrium.

The degree of the CNF dispersions in the water phase has to be considered for each system. The degree corresponds to the absorbance at 500 nm of a CNF suspension caused by the electronic transition of the CNFs (Bahr et al., 2001; Haiber et al., 2003). Figure 3 shows the 1-NP concentration dependence of the absorbance at 500 nm observed in the water suspension including 1-NP and the CNF samples. The degree of dispersion of the A1-CNF and A24-CNF increases with an increase in the concentration of 1-NP in contrast to the N-CNF. The A1-CNF and A24-CNF easily aggregate because of the hydrogen-bonding between the oxidized groups, whereas the results show that the adsorption of 1-NP on the groups effectively prevents the aggregation of the CNFs (Shaffer et al., 1998). Our study suggests that the oxidized groups promote the aggregation of the CNFs since the A1-CNF and A24-CNF are highly dispersed in basic solvents in which the oxidized groups are deprotonated.

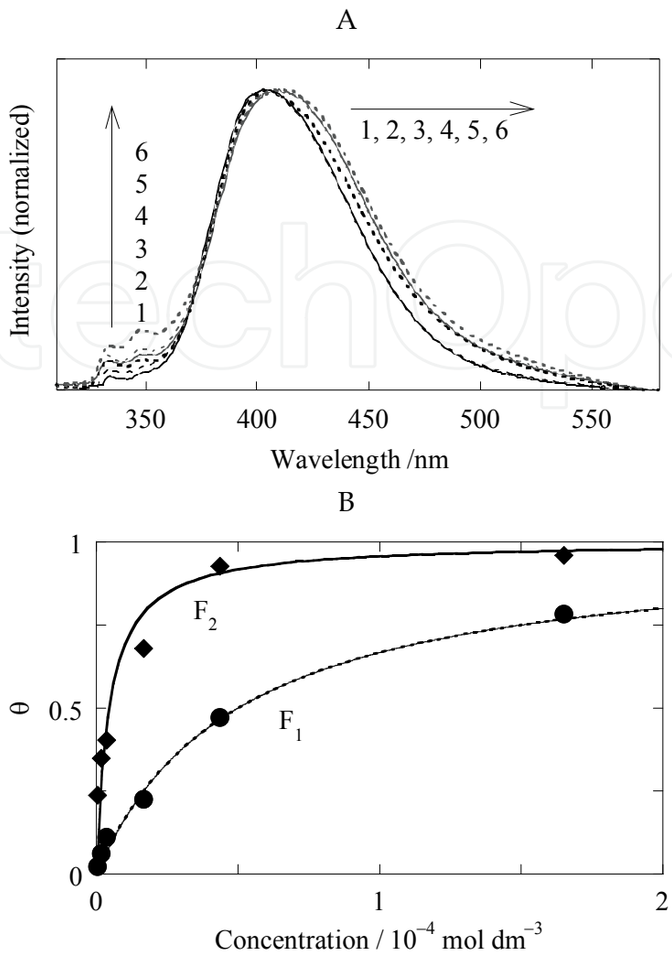

Fig. 2. (A) fluorescence spectra of 1-NP observed in aqueous suspension including A24-CNF and (B) resulting Langmuir isotherm for F_1 and F_2 sites. The initial concentrations of 1-NP in water are (1) 5.0×10^{-5}, (2) 8.0×10^{-5}, (3) 1.0×10^{-4}, (4) 2.0×10^{-4}, (5) 3.0×10^{-4}, and (6) 5.0×10^{-4} mol dm^{-3}. The excitation wavelength is 297 nm.

The average pK_a value of the groups, such as −COOH and −OH, on the CNFs was around 4.0, similar to that in a previous report (Toebes et al., 2004). The spectral data observed in the A1-CNF and A24-CNF systems shown in Figure 2 must be corrected with respect to the apparent amount of the dispersed CNFs. The intensities of the ^1L_b and the ion-pair fluorescences relative to that of the anion's were, therefore, reduced to the values per a certain amount of the CNFs corresponding to that of the dispersed N-CNF using the results shown in Figure 3.

Considering the ion-pair species of 1-NP interacting with the oxidized groups, IF, the total concentration of 1-NP, C, is given by

$$C = X[\mathrm{N}] + [\mathrm{IF}], \tag{5}$$

where

$$X = 1+[\mathrm{NF}]/[\mathrm{N}] = 1+AI_{\mathrm{NF}}/I_{\mathrm{N}}. \tag{6}$$

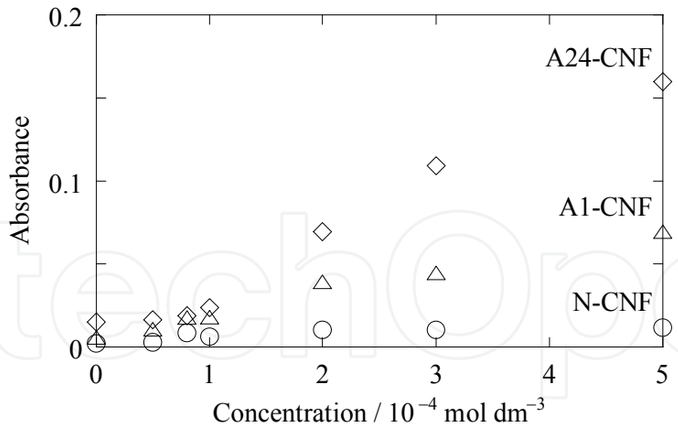

Fig. 3. 1-NP concentration dependence of absorbance at 500 nm observed in aqueous suspension including 1-NP and the N-CNF, A1-CNF, and A24-CNF.

The ratio of the fluorescence intensity of N, I_N, to that of IF, I_{IF}, is defined as R_2.

$$R_2 = I_N/I_{IF} = B[N]/[IF], \tag{7}$$

where B indicates the constant ratio of the fluorescence efficiency of N to that of IF defined similar to A.

$$B = \varepsilon_N \Phi_N / \varepsilon_{IF} \Phi_{IF}. \tag{8}$$

These equations can be adopted to the Langmuir isotherm as follows:

$$\theta = [IF]/[F_2] = K_2[N]/(1+ K_2[N]), \tag{9}$$

where F_2 is the adsorption site of the oxidized groups on the A1- or A24-CNF surface, and K_2 is the adsorption equilibrium constants on the F_2 sites. The $[F_2]$ value is the molar amount of the F_2 sites existing on the CNFs dispersed in 1 dm³ of water similar to $[F_1]$. The equilibrium equations for the site F_1 are also adopted for the A1-CNF and A24-CNF in order to estimate the values of $[F_1]$ and K_1. The values, $[F_1]$ and $[F_2]$, on the A1-CNF and A24-CNF are the corrected ones with respect to the amount of the dispersed CNFs.

The Langmuir isotherms of 1-NP on the surface of the A24-CNF for the F_2 sites were obtained by the curve fitting calculation using the variables, C, R_2, and X, and the parameters, B, K_2, and $[F_2]$. The isotherms for the F_1 site were also obtained in the same way for the N-CNF. The experimental and simulated relationships between the θ and [N] for the F_1 and F_2 sites are plotted in Figure 2B. The experimental values are well-fitted to the Langmuir isotherms. The constants for A1-CNF and A24-CNF are summarized in Table 1 in addition to those of N-CNF. The spectroscopic constants, A and B, are the magnitudes of the fluorescent quenching, so that a higher value means that the fluorescence is harder to be emitted. Our experimental results indicate that the F_1 site easily quenches the 1-NP fluorescence by about six times faster than the F_2 site. The value of K_2 is nearly 10 times higher than that of K_1, so that the interaction of the 1-NP molecules with the F_2 site is much larger than with the F_1 site. The relative amount of the F_2 sites to all the sites is 30% on the A1-CNF and 58% on the A24-CNF, indicating that the amount of oxidized groups increases with an increase in the acid treatment time. Considering that the N-CNF adsorbs a

naphthalene ring unit per 0.70 nm² based on a simulation of benzene molecules adsorbed on graphite (Vernov & Steele, 1991), we estimated the number of F_2 sites per nm² on the A1-CNF and A24-CNF as 0.46 and 1.18, respectively.

4. In situ probing of acidic groups on acid-treated carbon nanofibers using 1-aminopyrene

4.1 Changes in UV-visible absorption spectra of CNF suspensions

The N-, A24-, and AA-CNFs (0.50 mg) were individually dispersed in the 1-AP solutions (10 cm^3) containing water and ethanol (4/1 in volume) at 1.0×10^{-4} mol dm^{-3} by ultrasonic irradiation for 1−18 days. The resulting suspensions were centrifuged to remove any precipitates. The UV-visible absorption spectra of the resulting supernatant suspensions were measured in order to examine the adsorption of 1-AP on the CNFs and the dispersion of the CNFs into the liquid phase. The suspensions contained slightly amounts of acids and were almost neutral.

In the N-CNF suspension, only slight temporal changes in the spectrum are observed. This suggests that 1-AP was not adsorbed on the N-CNF surface as readily as 1-NP (Nishikiori et al., 2004; Kubota et al., 2005a). Our experiments revealed that the N-CNF clearly adsorbed pyrene better than 1-AP as shown in Figures 9A and 10A. This adsorption property indicates that the polar amino group prevents the π−π interaction between the pyrene ring and graphene sheet even though pyrene molecules are adsorbed onto the carbon nanotubes by this interaction (Chen et al., 2001a; Long & Yang, 2001). Figure 4 shows the absorption spectra of the AA-CNF suspension containing 1-AP observed immediately after the preparation, and after the ultrasonic irradiation for 4−11 days. In the AA-CNF and A24-CNF suspensions, the absorbance gradually decreases with time. We conclude from these data that there is an interaction between 1-AP and the acid-treated CNFs.

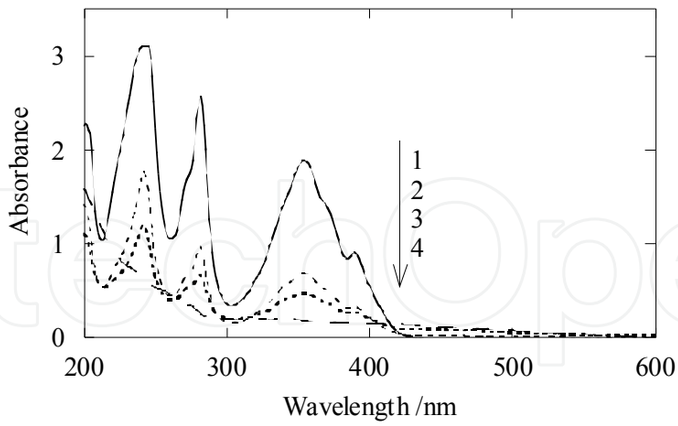

Fig. 4. Absorption spectra of AA-CNF suspensions containing 1-AP observed (1) just after the preparation and after ultrasonic irradiation of (2) 4, (3) 7, and (4) 11 days.

Figure 5 displays the changes in the absorbance of each CNF suspension at 350 and 500 nm versus the ultrasonic irradiation time. The absorbance at 350 nm indicates the amount of 1-AP existing in the liquid phase. 1-AP was hardly adsorbed on the N-CNF, but was adsorbed on both the A24-CNF and the AA-CNF. The AA-CNF was seen to adsorb the 1-AP at a faster rate than the A24-CNF. The absorbance at 500 nm corresponds to the degree of CNF

dispersion according to a good correlation between the concentration and the absorbance of the carbon nanotubes in a solvent (Bahr et al., 2001). Such nanocarbon materials exhibit the broad absorption spectra over a wide range of UV-visible-IR due to the superposition of various electric structures originating from many species (Saito et al., 1992; Saito et al., 2000). The wavelength of 500 nm was selected to observe the dispersion because 1-AP have no absorption at longer wavelength than around 450 nm and the CNFs have higher absorption at shorter wavelength. The absorbance increased with the ultrasonic irradiation time until reaching saturation. These results indicate that the degree of CNF dispersion of each sample is ordered in this way; AA-CNF, A24-CNF, N-CNF, with AA-CNF being most highly dispersed. This order is closely correlated to the amount of adsorbed 1-AP. In addition to the surface modification by the acid treatment the adsorption of aromatic molecules should also play an important role in the CNF dispersion (Kubota et al., 2005a).

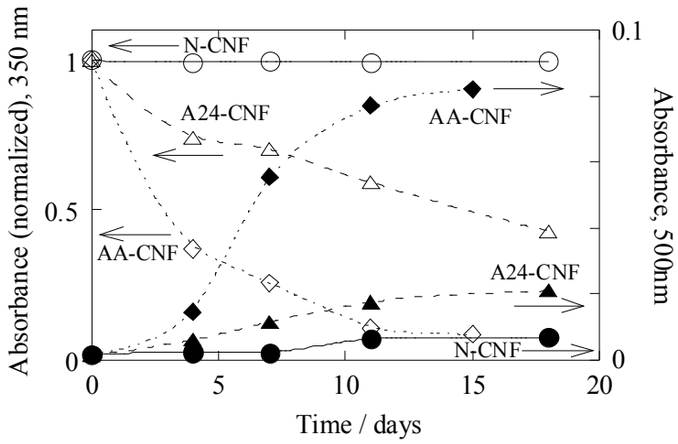

Fig. 5. Changes in absorbance vs. ultrasonic irradiation time monitored at 350 (open dots) and 500 nm (closed dots) in N-CNF, A24-CNF, and AA-CNF suspensions.

4.2 Changes in fluorescence and fluorescence excitation spectra of CNF suspensions

1-AP exhibits a protonation equilibrium; the original species is called AP, and the protonated species is called APH^+. The proton dissociation equilibrium constant of the ground state (pK_a) and the excited state (pK_a^*) are 2.8 and −1.2, respectively (Shizuka et al., 1979). Therefore, in moderately low-pH solutions, 1-AP exists as APH^+ in the ground state, deprotonates to form AP in the excited state, and then emits fluorescence.

Figure 6 shows the fluorescence and fluorescence excitation spectra of 1-AP in the AA-CNF suspension immediately after preparation and after ultrasonic irradiation for 4−11 days. The excitation wavelength for the fluorescence spectra was 350 nm, and the emission wavelength for the excitation spectra was 420 nm. The broad bands of fluorescence around 440 nm and fluorescence excitation around 350−400 nm are assigned to AP in the liquid phase of the suspension since they coincide with the spectra of 1-AP in neutral polar solvents (Hite et al., 1986; Miller et al., 2005). The shape of this excitation spectral band is also similar to that of the absorption spectra of 1-AP shown in Figure 4. The fluorescence spectral bands around 360−400 nm and fluorescence excitation spectra around 300−360 nm are similar to those of APH^+ in the acidic solution. Their relative intensities increased with ultrasonic irradiation time. The spectra of APH^+ are structurally similar to those of pyrene because the interaction between the free electron pair of nitrogen and the π-electrons in the

pyrene ring is blocked by protonation of the amino group (Hite et al., 1986; Miller et al., 2005). These results of the fluorescence indicate that 1-AP is adsorbed on the CNF surface to form APH^+-like species.

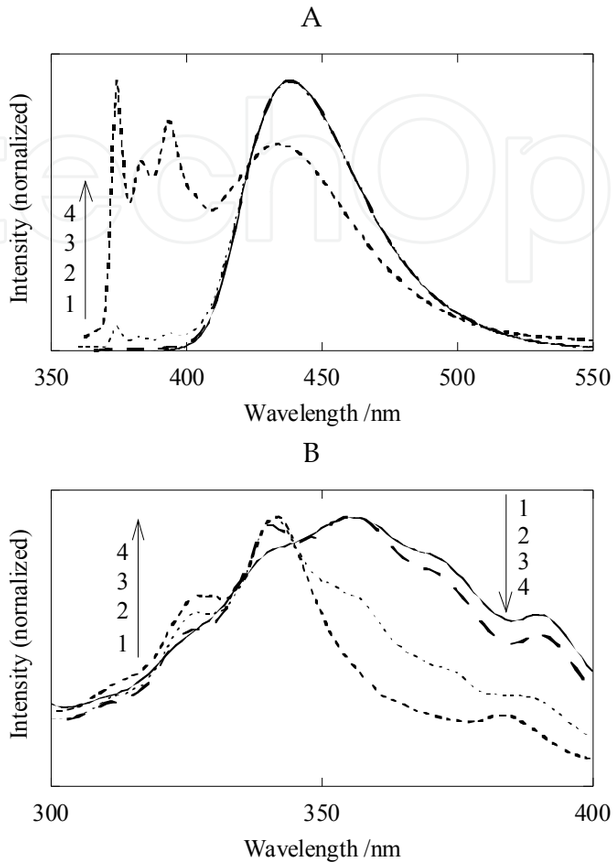

Fig. 6. (A) Fluorescence and (B) excitation spectra of 1-AP in AA-CNF suspension observed (1) just after the preparation and after ultrasonic irradiation of (2) 4, (3) 7, and (4) 11 days.

The ^1L_b fluorescence of 1-NP, which is observed in nonpolar environments, was seen on the CNFs due to π−π interaction between 1-NP and the graphene sheet (Nishikiori et al., 2004; Kubota et al., 2005a; Kubota et al., 2005b). The N-CNF cannot readily adsorb 1-AP molecules due to its low dispersibility throughout the solvent (Figure 6B). Some amount of 1-AP should be adsorbed onto the graphene sheet of the acid-treated CNFs because they are better dispersed throughout the liquid phase (Toebes et al., 2004; Lakshminarayanan et al., 2004). Unlike the 1-NP species, fluorescence was not observed, however, from the 1-AP species adsorbed through π−π interaction onto the CNFs. This is due to quenching that occurs in the more strongly interacting 1-AP/CNF systems.

Figure 7 shows the changes in the fluorescence intensities of 1-AP in the CNF suspensions as a function of the ultrasonic irradiation time. The fluorescence intensities of each CNF suspension at 375 nm per unit dispersed-CNF amount are plotted versus time. These values were obtained by dividing the original fluorescence intensities by the absorbance at 500 nm for each sample. The N-CNF did not adsorb 1-AP whereas the AA-CNF readily adsorbed 1-AP as the APH^+-like species. The A24-CNF adsorbed 1-AP at an intermediate rate. The

order of the adsorption ability of the CNF samples agreed with that estimated from the UV-visible absorption spectra depending on the CNF dispersion into the solvent.

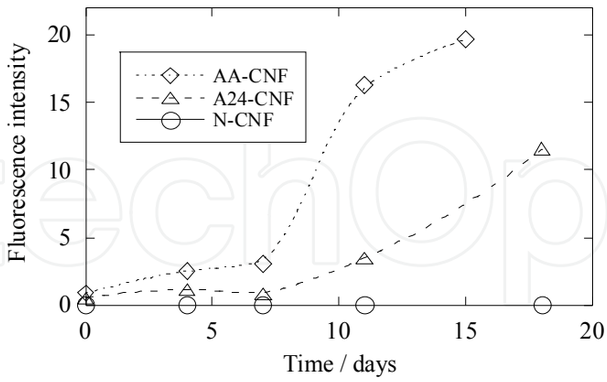

Fig. 7. Changes in fluorescence intensities of 1-AP per unit dispersed-CNF amount vs. ultrasonic irradiation time monitored at 375 nm in N-CNF (○), A24-CNF (Δ), and AA-CNF (◊) suspensions. The values were obtained by dividing the original fluorescence intensities by the absorbance at 500 nm for each sample.

The ion-pair fluorescence of 1-NP was generated by the relatively strong hydrogen-bonding between 1-NP and the oxidized groups, such as −COOH, −C=O, and −OH (Nishikiori et al., 2004; Kubota et al., 2005a). As a Brönsted base, 1-AP is expected to interact with the acidic oxygen-containing groups and selectively detected the acidic groups such as −COOH. It is suggested that 1-AP was immobilized by the hydrogen bonding between its amino group and the Brönsted-acidic groups on the CNF surface, leading to the formation of APH^+-like species. This behavior agrees with previously reported results that the carboxyl group on the carbon nanotube surface is modified by amines forming the ionic bond of $-COO^- {}^+H_3N-$ (Chen et al., 2001b; Kahn et al., 2002). The fluorescence intensities per unit dispersed-CNF amount for each CNF sample indicate that its adsorption ability depends on not only the CNF dispersion into the solvent but also the amounts of the acidic groups on the CNFs.

4.3 Confirmation of formation of APH^+-like species

The desorption of 1-AP from the AA-CNF surface was examined by fluorescence measurements in order to confirm the adsorption of 1-AP on the CNFs as shown in Figure 8. Figure 8A shows the fluorescence spectra of 1-AP in the AA-CNF suspension observed before and after adding sodium hydroxide. The fluorescence of the APH^+-like species was seen in the original suspension even though the suspension is nearly neutral. After adding the basic NaOH, the structural band of the fluorescence spectra disappeared. This result indicates that the 1-AP molecules that were adsorbed onto the CNF surface as the APH^+-like species were desorbed from the surface into the liquid phase. The APH^+-like species and the acidic groups should be deprotonated and would then hardly interact with one another since the pH value in the suspension was greater than 13. The adsorption and desorption equilibrium was shifted to the desorption process under this condition.

We examined the changes in the fluorescence spectra of the suspension re-dispersing the 1-AP-adsorbing AA-CNF as shown in Figure 8B. The suspension of the 1-AP-adsorbing AA-CNF was filtered, and then re-dispersed into pure water. The APH^+-like band intensity decreased with time while the AP band intensity increased with time. This result indicates

that a portion of the 1-AP molecules that were adsorbed onto the CNF surface as an APH^+-like species were desorbed from the surface and then diffused into the liquid phase. The results shown in Figure 8 support the adsorption of 1-AP onto the CNF surfaces as an APH^+-like species.

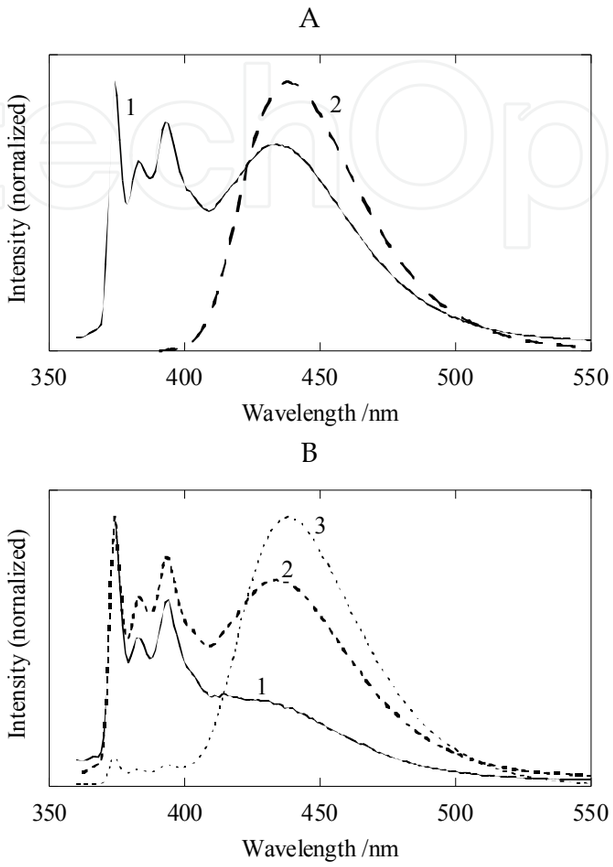

Fig. 8. Fluorescence spectra of 1-AP (A) in AA-CNF suspension observed before (1) and after (2) adding sodium hydroxide and (B) in suspension re-dispersing the 1-AP-adsorbing AA-CNF observed after ultrasonic irradiation of (1) 1, (2) 2, and (3) 5 h.

A stronger acid treatment caused the chemical modification to generate higher amounts of the acidic functional groups on the CNF surface. For this reason the more strongly treated CNFs (AA-CNF) was better dispersed in the 1-AP solution and adsorbed a higher amount of 1-AP than the weakly treated CNFs (A24-CNF). The quantitative analysis of the adsorption sites is now in progress and will be completed in the near future.

5. Fluorescence observation of pyrene adsorbed on carbon nanofibers

5.1 Changes in UV-visible absorption spectra of CNF suspensions

The N- or AA-CNF (0.50 mg) was individually dispersed in the pyrene solutions (10 cm^3) containing water and ethanol (4/1 in volume) at 1.0×10^{-5} mol dm^{-3} by ultrasonic irradiation for 1−8 days. The resulting suspensions were centrifuged to remove any precipitates.

The adsorption of pyrene on the CNF surface and the dispersion of the CNFs into the liquid phase were examined by UV-visible absorption of the CNF suspensions. Figure 9 shows the

absorption spectra of the N-CNF and AA-CNF suspensions containing pyrene observed just after the preparation (day 0) and after ultrasonic irradiation for several days. The absorption spectrum of the N-CNF suspension as prepared, which ranges around 220−350 nm, is almost same as that of pyrene in the water/ethanol solution. The absorbance of pyrene gradually decreased with the ultrasonic irradiation time due to its adsorption onto the N-CNF. The N-CNF was obviously found to adsorb pyrene (Chen et al., 2001; Tomonari et al., 2006) similar to 1-NP (Nishikiori et al., 2004; Kubota et al., 2005a). In the AA-CNF suspension, even the absorbance observed just after the preparation was lower than that in the solution, and the absorbance progressively decreases at a faster rate than in the N-CNF suspension. The ultrasonic irradiation makes the CNF bundles disentangled and dispersed into the liquid phase, and then the number of collision of the CNFs with pyrene molecules increases. Oxygen-containing functional groups on the surface of the acid-treated CNFs prevent the π−π interaction between the CNF graphene sheets and interact with solvents (Nishikiori et al., 2004; Kubota et al., 2005a; Kubota et al., 2005b). Therefore, the more highly dispersed AA-CNF was suggested to adsorb a higher amount of pyrene than the low dispersed N-CNF.

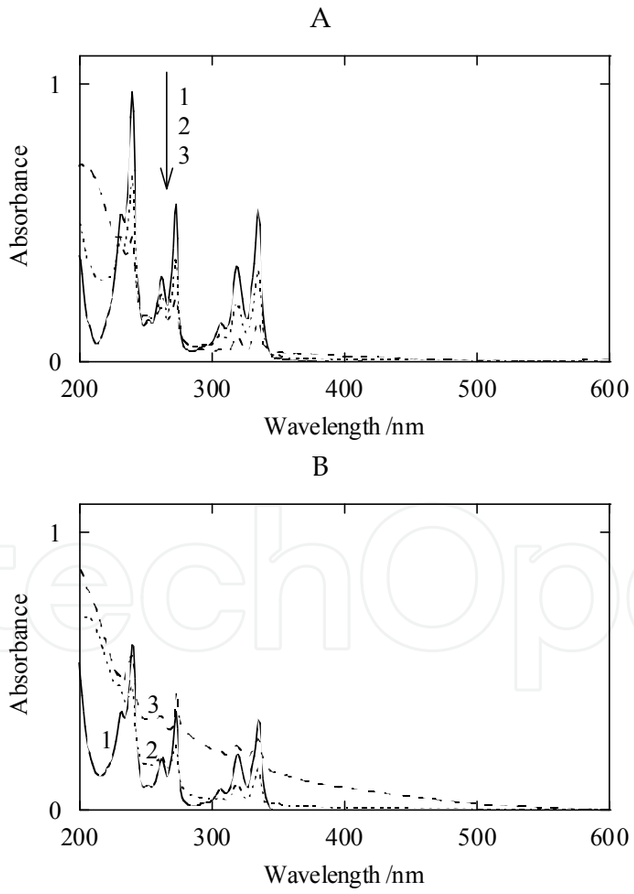

Fig. 9. Absorption spectra of (A) N-CNF and (B) AA-CNF suspensions containing pyrene; (A) (1) just after the preparation and after ultrasonic irradiation of (2) 2 and (3) 5 days, (B) (1) just after the preparation and after ultrasonic irradiation of (2) 1 and (3) 3 days.

Figure 10 shows the changes in the absorbance of each CNF suspension at 334 and 500 nm versus the ultrasonic irradiation time. The absorbance at 334 nm reflects the amount of pyrene existing in the liquid phase. The absorbance of pyrene in the solution without CNFs was also denoted by the closed circles located at day 0. However, unlike the N-CNF suspension, the spectra of the AA-CNF suspension include the strong absorption of the dispersed CNFs in the wavelength region of pyrene absorption. The net pyrene absorbance was obtained by subtracting the CNF absorption spectra from the original ones. The absorbance of pyrene in the solution before adding the CNFs was 0.52. The absorbance of pyrene in the N-CNF suspension, which was 0.52 at day 0, decreased with the irradiation time due to its adsorption. The adsorption equilibrium on the N-CNF was almost reached after the 5-days irradiation, when the absorbance was 0.12. This result indicates that the concentration of pyrene in the liquid phase decreased until reaching saturation. The AA-CNF was seen to adsorb the pyrene at a faster rate than the N-CNF. The absorbance of pyrene in the AA-CNF suspension, which was 0.33 at day 0, decreased with the irradiation time until reaching saturation after the 3-days irradiation, when the absorbance was 0.043.

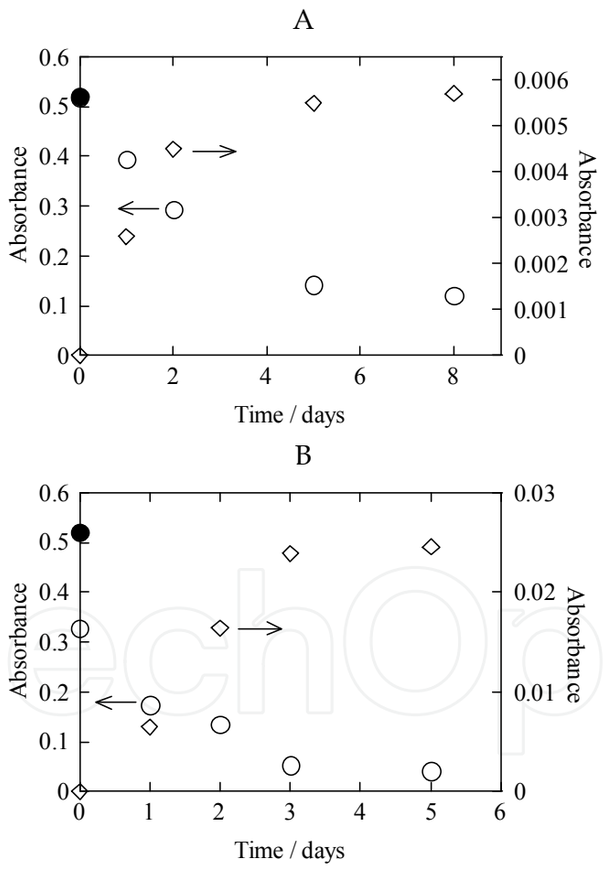

Fig. 10. Changes in absorbance vs. ultrasonic irradiation time monitored at 334 (○) and 500 (◊) nm in (A) N-CNF and (B) AA-CNF suspensions. The closed circles at day 0 denote the absorbance of pyrene in the solution.

The absorbance at 500 nm corresponds to the degree of CNF dispersion according to a good correlation between the concentration and the absorbance of the CNTs in a solvent (Bahr et

al., 2001). Such nanocarbon materials exhibit the broad absorption spectra over a wide range of UV-visible-IR due to the superposition of various electric structures originating from many species, regardless of whether they are acid-treated or not. The each absorbance of the N-CNF and AA-CNF suspensions, which was almost zero at day 0, increased with the ultrasonic irradiation time and reached saturation after the 5- and 3-days irradiation, respectively. The absorbance values of the N-CNF and AA-CNF suspensions at the dispersion saturation were 0.0057 and 0.025, respectively. These results indicate that the dispersion of the AA-CNF is higher than that of N-CNF due to the functional groups produced on the CNF surface by the acid treatment and it is closely correlated to the amount of the adsorbed pyrene.

5.2 Changes in fluorescence spectra of CNF suspension

It is well known that the ratio of vibronic peak intensities in fluorescence spectra of pyrene changes with the surrounding polarity (Nakajima, 1971; Kalyanasundaram & Thomas, 1977). Therefore, pyrene is available to use as an in-situ probe of polarity in the surrounding media.

Figure 11 shows the fluorescence spectra of pyrene in the N-CNF and AA-CNF suspensions observed just after the preparation (day 0) and after ultrasonic irradiation for 1−5 days compared with that in cyclohexane. The excitation wavelength for the fluorescence spectra was 350 nm in the weak ^1L_b (S_1) band of pyrene. The emission wavelength for the excitation spectra was 392 nm. The fluorescence peaks at 372, 382, and 392 nm observed at day 0 are assigned to pyrene present in liquid phase of the suspension. The intensity of the 0−0 vibronic bands is significantly enhanced at the expense of other bands in the polar solvents due to solute−solvent dipole−dipole interaction (Nakajima, 1971; Kalyanasundaram & Thomas, 1977). The relative peak intensity at 372 nm to that at 382 nm decreased with the ultrasonic irradiation time in both the N-CNF and AA-CNF systems, and the spectrum became a feature similar to that observed in non-polar solvent such as cyclohexane. These results indicate that pyrene is absorbed on graphene sheet of the CNF surface by the π−π interaction similar to 1-NP (Nishikiori et al., 2004; Kubota et al., 2005a; Kubota et al., 2005b). Although such fluorescence was easily quenched by a much stronger π−π interaction, the spectrum was clearly observed in our systems due to the highly dispersion system of the CNFs throughout the solution. The AA-CNF is oxidized on only a small part of the surface and has a relatively large area of the unoxidized low-polar surface. The fluorescence spectra indicate that pyrene molecules are adsorbed on the low-polar area of the graphene sheet of both the N-CNF and AA-CNF.

The excitation spectra of the samples were also measured and obtained the peaks at 320 and 335 nm corresponding to the ^1L_a absorption and the weak band at 350−380 nm corresponding to the ^1L_b absorption. As shown in Figure 12, it was barely found that the relative peak intensity at 372 nm (0−0 band) to that at 361 nm for the AA-CNF system decreased with the ultrasonic irradiation time (Nakajima, 1971).

Figure 13 shows the changes in ratio of the fluorescence intensity of the pyrene in the CNF suspensions at 372 nm to that at 382 nm as a function of the ultrasonic irradiation time. The fluorescence intensity ratio for the CNF suspension containing pyrene before ultrasonic irradiation (day 0) is 1.6, which is confirmed to be same as that of pyrene in the water/ethanol solution (4/1 in volume) although the results are not shown here. Both the ratios for the N-CNF and AA-CNF suspensions decreased with the ultrasonic irradiation time and then were 0.77 after 5-days irradiation and 0.76 after 3-days irradiation,

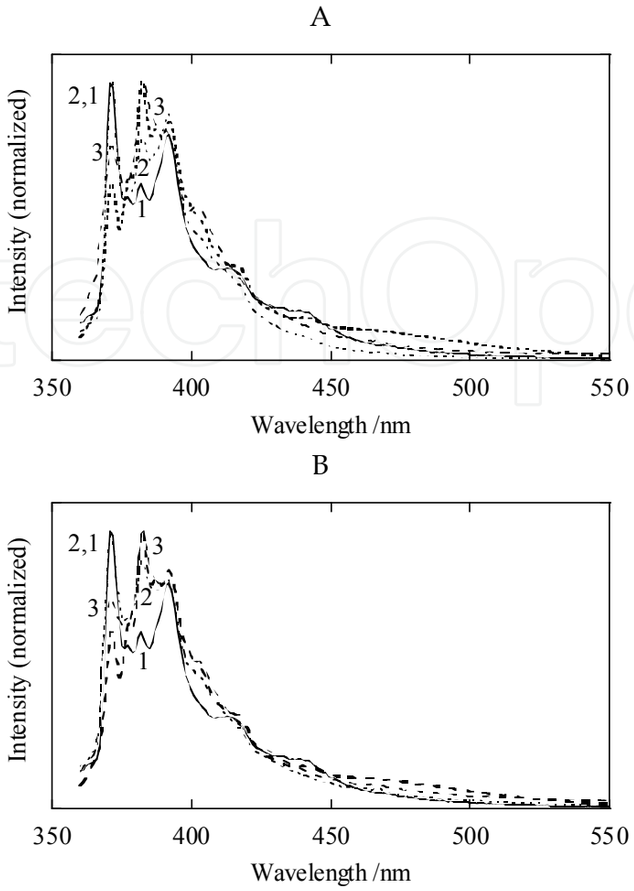

Fig. 11. Fluorescence spectra of pyrene in (A) N-CNF and (B) AA-CNF suspensions upon 350 nm excitation; (a) (1) just after the preparation and after ultrasonic irradiation of (2) 2 and (3) 5 days, (b) (1) just after the preparation and after ultrasonic irradiation of (2) 1 and (3) 3 days. Bold broken lines indicate fluorescence spectra of pyrene in cyclohexane.

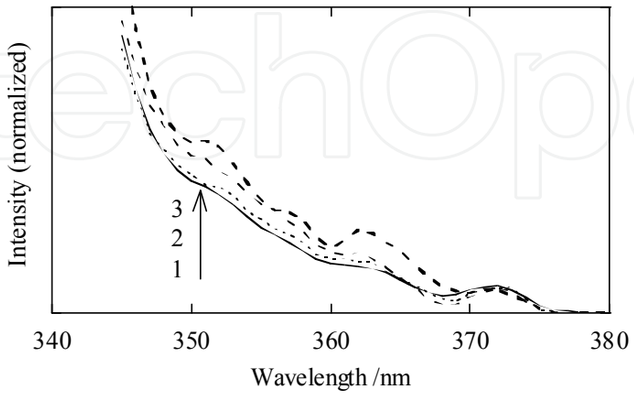

Fig. 12. Fluorescence excitation spectra of pyrene in AA-CNF suspension monitored at 392 nm; (1) just after the preparation and after ultrasonic irradiation of (2) 1 and (3) 3 days. Bold broken line indicates spectrum of pyrene in cyclohexane.

respectively, when they reached the constant values. They became close to the value in cyclohexane as a non-polar solvent, 0.63. Therefore, pyrene molecules were adsorbed onto the low-polar surface of the CNF graphene sheet by π−π interaction. Obviously, the adsorption of pyrene onto the AA-CNF reached its equilibrium earlier than that onto the N-CNF due to the higher dispersion of CNFs throughout the solution. The changes in the fluorescence intensity during ultrasonic irradiation well-corresponded to those in the CNF dispersion throughout the solutions and the pyrene adsorption onto the CNFs.

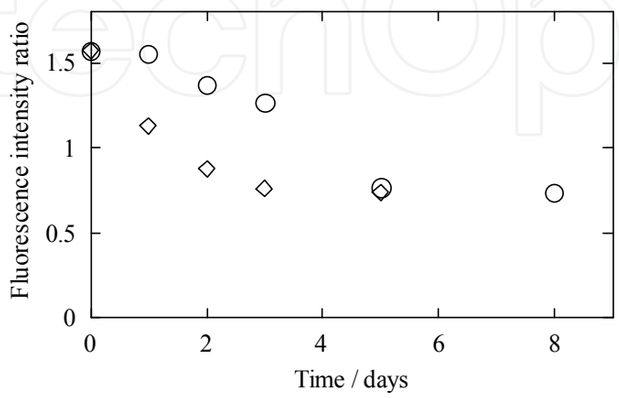

Fig. 13. Changes in ratio of fluorescence intensity of pyrene at 372 nm to that at 382 nm in N-CNF (○) and AA-CNF (◊) suspensions vs. ultrasonic irradiation time.

6. Conclusions

A unique procedure to create a highly disperse system of CNFs throughout solvents allows in situ fluorescence measurements using aromatic probe molecules even though the fluorescence of those adsorbed on carbon materials is scarcely observed due to strong quenching.

Oxidized groups on the outer surface of acid-treated CNFs are quantified using 1-naphthol (1-NP), whereas it is difficult to obtain quantitative information of the chemical species existing in a monolayer or only a few layers of the oxidized surface of the CNFs by IR spectroscopy. In situ fluorescence measurements of CNFs using 1-NP revealed two types of adsorption onto the surface of the CNFs when they were dispersed in solvents. One is generated by the π−π interaction between 1-NP and the graphene sheet and the other is the hydrogen-bonding interaction between 1-NP and proton-accepting groups such as −COOH (−COO^-) and −C=O.

Furthermore, acidic functional groups such as −COOH produced on the surface of acid-treated CNFs are characterized using 1-aminopyrene (1-AP) as a Brönsted base. The 1-AP molecules only slightly interact with the untreated CNF surface, whereas the 1-AP cation-like bands are observed on the acid-treated CNF surfaces. These results indicate that 1-AP is tightly immobilized by the hydrogen bonding interaction between its amino group and the Brönsted-acidic groups on the CNF surface.

However, unlike the 1-NP species, the low-polar species fluorescence is not observed from the 1-AP species on the graphene sheet of the CNFs. This is because the polar amino group prevents the π−π interaction between the pyrene ring and graphene sheet. The fluorescence spectra of pyrene as observed in low-polar solvents are clearly found in the suspensions

containing pyrene and the CNFs due to its adsorption onto the CNF graphene sheet by π−π interaction. The CNF dispersion well-corresponds to the adsorption of pyrene onto the CNF surface.

In situ fluorescence measurements using aromatic probe molecules are useful for studying the physicochemical properties on the CNF surface.

7. Acknowledgements

This work was supported by the CLUSTER of the Ministry of Education, Culture, Sports, Science and Technology.

8. References

Bahr, J. L.; Mickelson, E. T.; Bronikowski, M. J.; Smalley, R. E. & Tour, J. M. (2001). Dissolution of small diameter single-wall carbon nanotubes in organic solvents? *Chem. Commun.*, 2001, 2, 193−194.

Chen, R. J.; Zhang, Y.; Wang, D. & Dai, H. (2001a). Noncovalent sidewall functionalization of single-walled carbon nanotubes for protein immobilization. *J. Am. Chem. Soc.*, 123, 16, 3838−3839.

Chen, J.; Rao, A. M.; Lyuksyutov, S.; Itkis, M. E.; Hamon, M. A.; Hu, H.; Cohn, R. W.; Eklund, P. C.; Colbert, D. T.; Smalley, R. E. & Haddon, R. C. (2001b). Dissolution of full-length single-walled carbon nanotubes. *J. Phys. Chem. B*, 105, 13, 2525−2528.

Endo, M. (1988). Grow carbon fibers in the vapor phase. *CHEMTECH*, 18, 9, 568−576.

Endo, M.; Kim, Y. A.; Hayashi, T.; Nishimura, K.; Matsushita, T. & Dresselhaus, M. S. (2001). Vapor-grown carbon fibers (VGCFs): Basic properties and their battery applications. *Carbon*, 39, 9, 1287−1297.

Endo, M.; Kim, Y.A.; Fukai, T.; Hayashi, T.; Oshida, K.; Terrones, M.; Yanagisawa, T.; Higaki, S. & Dresselhaus, M. S. (2002). Structural characterization of cup-stacked-type nanofibers with an entirely hollow core. *Appl. Phys. Lett.*, 80, 7, 1267−1269.

Fujii, T.; Mabuchi, T.; Kitamura, H.; Kawauchi, O.; Negishi, N. & Anpo, M. (1992). Fluorescence spectra of 1-naphthol during the sol-gel process of a mixed aluminum-silicon alkoxide (Si : Al = 94 : 6). *Bull. Chem. Soc. Jpn.*, 65, 3, 720−727.

Fujii, T.; Sugawara, Y.; Kodaira, K.; Mabuchi, T. & Anpo, M. (1995). Characteristic changes in the fluorescence spectra of 1-naphthol at the gelation point during the sol-gel-xerogel transitions. *Res. Chem. Intermed.*, 21, 6, 643−652.

Gao, J.; Itkis, M. E.; Yu, A.; Bekyarova, E.; Zhao, B. & Haddon, R. C. (2005). Continuous spinning of a single-walled carbon nanotube−nylon composite fiber. *J. Am. Chem. Soc.*, 127, 11, 3847−3854.

Hamon, M. A.; Hu, H.; Bhowmik, P.; Niyogi, S.; Ahao, B.; Itkis, M. E. & Haddon, R. C. (2001). End-group and defect analysis of soluble single-walled carbon nanotubes. *Chem. Phys. Lett.*, 347, 1−3, 8−12.

Hamon, M. A.; Hui, H.; Bhowmik, P.; Itkis, H. M. E. & Haddon, R. C. (2002). Ester-functionalized soluble single-walled carbon nanotubes. *Appl. Phys. A*, 74, 3, 333−338.

Hite, P.; Krasnansky, R. & Thomas, J. K. (1986). Spectroscopic investigations of surfaces by using aminopyrene. *J. Phys. Chem.*, 90, 22, 5795−5799.

Hongbing, Z.; Wenzhe, C.; Minquan, W.; Zhengchan & Chunlin, Z. (2004). Optical limiting effects of multi-walled carbon nanotubes suspension and silica xerogel composite. *Chem. Phys. Lett.*, 382 313−317.

Iijima, S. (1991). Helical microtubules of graphitic carbon. *Nature*, 354, 6348, 56−58.

Iijima, S. & Ichihashi, T. (1993). Single-shell carbon nanotubes of 1-nm diameter. *Nature*, 363, 6430, 603−605.

Kahn, M. G.; Banerjee, S. & Wong, S. S. (2002). Solubilization of oxidized single-walled carbon nanotubes in organic and aqueous solvents through organic derivatization. *Nano Lett.*, 2, 11, 1215−1218.

Kalyanasundaram, K. & Thomas, J. K. (1977). Environmental effects on vibronic band intensities in pyrene monomer fluorescence and their application in studies of micellar systems. *J. Am. Chem. Soc.*, 99, 7, 2039−204.

Kubota, S.; Nishikiori, H.; Tanaka, N.; Endo, M. & Fujii, T. (2005a). Quantitative characterization of surface adsorption sites of carbon nanofibers by in-situ fluorescence measurement using 1-naphthol. *Chem. Phys. Lett.*, 412, 1−3, 223−227.

Kubota, S.; Nishikiori, H.; Tanaka, N.; Endo, M. & Fujii, T. (2005b). Dispersion of acid-treated carbon nanofibers into gel matrices prepared by the sol−gel method. *J. Phys. Chem. B*, 109, 43, 23170−23174.

Lakshminarayanan, P. V.; Toghiani, H. & Pittman Jr., C. U. (2004). Nitric acid oxidation of vapor grown carbon nanofibers. *Carbon*, 42, 12−13, 2433−2442.

Liu, J.; Rinzer, G.; Dai, H.; Hafner, J. H.; Bradley, R. K.; Boul, P. J.; Lu, A.; Iverson, T.; Shelimov, K.; Huffman, C. B.; Rodriguez-Macias, F.; Shon, Y. S.; Lee, T. R.; Colbert, D. T. & Smalley, R. E. (1998). Fullerene Pipes. *Science*, 280, 5367, 1253−1256.

Long, R. Q. & Yang, R. T. (2001). Carbon nanotubes as superior sorbent for dioxin removal. *J. Am. Chem. Soc.*, 123, 9, 2058−2059.

Miller, E.; Wysocki, S. & Jóźwik, D. (2005). Fluorescence studies of the sol–gel transition using aminopyrene. *J. Photochem. Photobiol. A*, 169, 3, 221−228.

Nakajima, A. (1971). Solvent effect on the vibrational structures of the fluorescence and absorption spectra of pyrene. *Bull. Chem. Soc. Jpn.*, 44, 12, 3272−3277.

Nishikiori, H.; Tanaka, N.; Kubota, S.; Endo, M. & Fujii, T. (2004). In situ characterization of surface physicochemical properties of carbon nanofibers using 1-naphthol as a fluorescent probe. *Chem. Phys. Lett.*, 390, 4−6, 389−393.

Nishikiori, H.; Tanaka, N.; Tanigaki, T.; Endo, M. & Fujii, T. (2008). In situ probing of acidic groups on acid-treated carbon nanofibers using 1-aminopyrene. *J. Photochem. Photobiol. A*, 193 2−3, 161−165.

Oberlin, A.; Endo, M. & Koyama, T. (1976). Filamentous growth of carbon through benzene decomposition. *J. Cryst. Growth.*, 32, 3, 335−249.

Park, C.; Ounaies, Z.; Watson, K. A.; Crooks, R. E.; Smith, J.; Lowther, S. E.; Connell, J. W.; Siochi, E. J.; Harrison, J. S. & St. Clair, T. L. (2002). Dispersion of single wall carbon nanotubes by in situ polymerization under sonication. *Chem. Phys. Lett.*, 364, 3−4, 303−308.

Saito, R.; Fujita, M.; Dresselhaus, G. & Dresselhaus, M. S. (1992). Electronic structure of chiral graphene tubules. *Appl. Phys. Lett.*, 60, 18, 2204−2207.

Saito, R.; Dresselhaus, G. & Dresselhaus, M. S. (2000). Trigonal warping effect of carbon nanotubes. *Phys. Rev. B*, 61, 4, 2981−2990.

Shizuka, H.; Tsutsumi, K.; Takeuchi, H. & Tanaka, I. (1979). Direct measurement of proton dissociation in thhe excited state of protonated 1-aminopyrene with picosecond pulses. Chem. Phys. Lett., 62, 2, 408−411.

Singh, R.; Pantarotto, D.; McCarthy, D.; Chaloin, O.; Hoebeke, J.; Partidos, C. D.; Briand, J. P.; Prato, M.; Bianco, A. & Kostarelos, K. (2005). Binding and condensation of plasmid dna onto functionalized carbon nanotubes: Toward the construction of nanotube-based gene delivery vectors. *J. Am. Chem. Soc.*, 127, 12, 4388−4396.

Suzuki, S.; Fujii, T.; Imai, A. & Akahori, H. (1977). The fluorescent level inversion of dual fluorescences and the motional relaxation of excited state molecules in solutions. *J. Phys. Chem.*, 81, 16, 1592−1598.

Tan, T. T.; Sim, H. S.; Lau, S. P.; Yang, H. Y.; Tanemura, M. & Tanaka, J. (2006). X-ray generation using carbon-nanofiber-based flexible field emitters. *Appl. Phys. Lett.*, 88, 10, 103105.

Tanigaki, T.; Nishikiori, H.; Kubota, S.; Tanaka, N.; Endo, M. & Fujii, T. (2007). Fluorescence observation of pyrene adsorbed on carbon nanofibers. *Chem. Phys. Lett.*, 448, 4−6, 218−222.

Toebes, M. L.; van Heeswijk, J. M. P.; Bitter, J. H.; Jos van Dillen, A. & de Jong, K. P. (2004). The influence of oxidation on the texture and the number of oxygen-containing surface groups of carbon nanofibers. *Carbon*, 42, 2, 307−315.

Tomonari, Y.; Murakami, H. & Nakashima, N. (2006). Solubilization of single-walled carbon nanotubes by using polycyclic aromatic ammonium amphiphiles in water—strategy for the design of high-performance solubilizers. *Chem. Eur. J.*, 12, 15, 4027−4034.

Wang, F.; Arai, S. & Endo,M. (2005). Preparation of nickel–carbon nanofiber composites by a pulse-reverse electrodeposition process. *Electrochem. Commun.*, 7, 7, 674−678.

Yang, X.; Guillorn, M. A.; Austin, D.; Melechko, A. V.; Cui, H.; Meyer III, H. M.; Merkulov, V. I.; Caughman, J. B. O.; Lowndes, D. H. & Simpson, M. L. (2003). Fabrication and characterization of carbon nanofiber-based vertically integrated schottky barrier junction diodes. *Nano Lett.*, 3, 12, 1751−1755.

Zhu,J.; Kim, J. D.; Peng, H.; Margrave, J. L.; Khabashesku, V. N. & Barrera, E. V. (2003). Improving the dispersion and integration of single-walled carbon nanotubes in epoxy composites through functionalization. *Nano Lett.*, 3, 8, 1107−1113.

Nanofibers

Edited by Ashok Kumar

ISBN 978-953-7619-86-2
Hard cover, 438 pages
Publisher InTech
Published online 01, February, 2010
Published in print edition February, 2010

“There’s Plenty of Room at the Bottom” this was the title of the lecture Prof. Richard Feynman delivered at California Institute of Technology on December 29, 1959 at the American Physical Society meeting. He considered the possibility to manipulate matter on an atomic scale. Indeed, the design and controllable synthesis of nanomaterials have attracted much attention because of their distinctive geometries and novel physical and chemical properties. For the last two decades nano-scaled materials in the form of nanofibers, nanoparticles, nanotubes, nanoclays, nanorods, nanodisks, nanoribbons, nanowhiskers etc. have been investigated with increased interest due to their enormous advantages, such as large surface area and active surface sites. Among all nanostructures, nanofibers have attracted tremendous interest in nanotechnology and biomedical engineering owing to the ease of controllable production processes, low pore size and superior mechanical properties for a range of applications in diverse areas such as catalysis, sensors, medicine, pharmacy, drug delivery, tissue engineering, filtration, textile, adhesive, aerospace, capacitors, transistors, battery separators, energy storage, fuel cells, information technology, photonic structures and flat panel displays, just to mention a few. Nanofibers are continuous filaments of generally less than about 1000 nm diameters. Nanofibers of a variety of cellulose and non-cellulose based materials can be produced by a variety of techniques such as phase separation, self assembly, drawing, melt fibrillation, template synthesis, electro-spinning, and solution spinning. They reduce the handling problems mostly associated with the nanoparticles. Nanoparticles can agglomerate and form clusters, whereas nanofibers form a mesh that stays intact even after regeneration. The present book is a result of contributions of experts from international scientific community working in different areas and types of nanofibers. The book thoroughly covers latest topics on different varieties of nanofibers. It provides an up-to-date insightful coverage to the synthesis, characterization, functional properties and potential device applications of nanofibers in specialized areas. We hope that this book will prove to be timely and thought provoking and will serve as a valuable reference for researchers working in different areas of nanofibers. Special thanks goes to the authors for their valuable contributions.

How to reference

In order to correctly reference this scholarly work, feel free to copy and paste the following:

Hiromasa Nishikiori, Satoshi Kubota, Nobuaki Tanaka, Morinobu Endo, and Tsuneo Fujii (2010). In Situ Probing of Oxygen-Containing Groups on Acid-treated Carbon Nanofibers using Aromatic Molecules, Nanofibers, Ashok Kumar (Ed.), ISBN: 978-953-7619-86-2, InTech, Available from: http://www.intechopen.com/books/nanofibers/in-situ-probing-of-oxygen-containing-groups-on-acid-treated-carbon-nanofibers-using-aromatic-molecul

INTECH
open science | open minds

InTech Europe
University Campus STeP Ri
Slavka Krautzeka 83/A
51000 Rijeka, Croatia
Phone: +385 (51) 770 447
Fax: +385 (51) 686 166
www.intechopen.com

InTech China
Unit 405, Office Block, Hotel Equatorial Shanghai
No.65, Yan An Road (West), Shanghai, 200040, China
中国上海市延安西路65号上海国际贵都大饭店办公楼405单元
Phone: +86-21-62489820
Fax: +86-21-62489821

IntechOpen